Experimental and Numerical Investigation of a Pressure Swirl Atomizer

B. Sumer*, N. Erkan*, O. Uzol+, I.H.Tuncer+
* Defense Industries Research and Development Institute, Scientific and Technological Research Council of Turkey (TÜBİTAK-SAGE), Ankara, Turkey.
+Department of Aerospace Engineering, Middle East Technical University, Ankara, Turkey.
bulent.sumer@tubitak.gov.tr, nejdeterkan@gmail.com, uzol@metu.edu.tr, tuncer@ae.metu.edu.tr

Abstract

The flow structure inside a pressure swirl atomizer is investigated using high-speed shadowgraphy techniques and computational fluid dynamics tools. The hollow cone spray properties are detected using Phase Doppler Particle Analyzer. The experimental and numerical results are analyzed and compared. The aircore inside the pressure swirl atomizer is visualized at high temporal and spatial resolutions with the high-speed shadowgraphy system. The images captured are analyzed quantitatively with a developed image processing tool. The analyses reveal strong fluctuations of the aircore diameter. Three dimensional and two dimensional axisymmetric-swirl models are used for the numerical study performed with ANSYS-FLUENT software. Unsteady, two phase laminar flows are computed using the volume of fluid method. Three-dimensional and two-dimensional numerical simulations also predict strong oscillations of aircore diameter near the base of swirl chamber. In addition, a two-component Phase Doppler Particle Analyzer is employed to investigate the spray properties.

Introduction

The combustion of liquid fuels is dependent on effective atomization to increase the surface area of the fuel and thereby achieve high rates of mixing and evaporation [1]. Pressure swirl atomizers are found to be the inexpensive and most reliable type of atomizer for fuel injection due to its superior atomization characteristics and relatively simple geometry. The atomization characteristics of swirl atomizers offer a significant advantage in throttling and give high thrust per atomizer [2]. They are less sensitive to manufacturing processes, chocking and cavitations when compared to plain orifice atomizers. They also have self tuning capability with variable flow resistance under transient conditions which improves the engine start up operations. The pressure swirl atomizers, in general, produce a hollow cone spray without the presence of liquid jet along the axis of the atomizer. This property of the hollow cone spray has the advantage of recirculating the hot combustion products to the atomizer exit to stabilize the flame and protecting the wall of the injector plate from excessive heat in liquid rocket engines [3].

In pressure swirl atomizers the propellant is fed through the tangential inlet passages into the swirl chamber. A liquid vortex with a free surface is formed within the atomizer. The radius of the free surface changes from minimum at the base of the swirl chamber to a larger value at the exit of the nozzle. A thinner liquid film exits through the nozzle and eventually breaks up into fine droplets forming a hollow cone spray (Figure 1a). Despite the geometric simplicity of the pressure swirl atomizer, the hydrodynamic processes occurring within the nozzle are highly complex. The formation of aircore within the atomizer makes the flow inside the atomizer a free surface flow. The highly complex hydrodynamic processes that occur in the swirl atomizer direct researchers to use simplified models. In the earlier analytical studies, the flow inside the swirl atomizer is treated as a steady, incompressible, inviscid flow [4-6]. In the recent experimental and numerical studies the formation of aircore inside the atomizer, the effect of various flow and geometrical parameters on aircore and the resulting spray characteristics are investigated [8-14]. The surface waves on the gas-liquid interface are identified and the resulting unsteady flow behavior is studied [15-18]. With the recent developments of measurement systems and computational tools including hardware and software, the researches on pressure swirl atomizers still continues and provide new insights into the flow through the atomizers and the phenomena of atomization [19-24].

In this paper, unsteady flows inside a pressure swirl atomizer, whose steady characteristics were studied previously by Dash et.al. [14], are first investigated experimentally with a high-speed shadowgraphy system. It provides large-amount of transient and fine-resolved data, which is then used to investigate highly transient two-

*Corresponding author: bulent.sumer@tubitak.gov.tr

phase fluid flow physics with statistical methods. The radial variation in Sauter mean diameter (SMD) is measured at one axial location with the Phase Doppler Particle Analyzer (PDPA) system. Furthermore, detailed numerical investigation of the unsteady flow inside the atomizer is performed in 2D and 3D using ANSYS-FLUENT Computational Fluid Dynamics (CFD) Software.

2. Experimental and Numerical Methods

Experimental Method

The internal geometry of the pressure swirl atomizer studied is given in Figure 1b. Pressure swirl atomizer is manufactured from Plexiglas in order to visualize the aircore inside the atomizer at high temporal and spatial resolutions. The experiments are performed with water at a constant flow rate of 3.18×10^{-3} m^3/min.

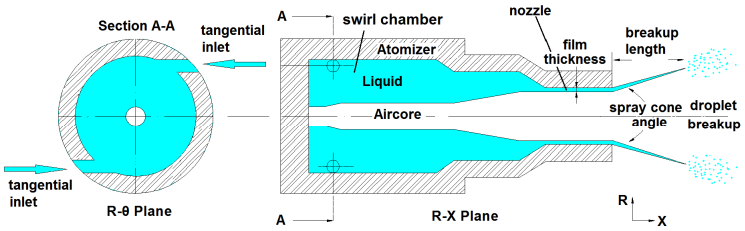

a

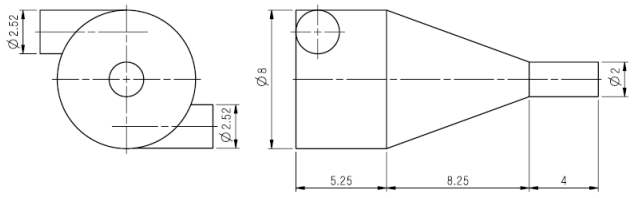

b

Figure1a. Flow through the pressure swirl atomizer and the hollow cone spray, **b.** Geometrical dimensions of the pressure swirl atomizer studied in the present study (all dimensions are in millimeters).

The atomizer test facility consists of a 40 liters water tank which can stand pressures up to 200 bars. An industrial type nitrogen cylinder, which is equipped with a pressure regulator, is used to pressurize the water tank to drive the water flow from tank to atomizer. A needle valve controls the flow rate of water to the atomizer. A turbine type flow meter measures the water flow rate, which has an error value of 0.75% at the flow rate considered. Main line from the water tank branches into two after the flow meter and water is fed into the atomizer from two tangential inlet passages. Both branches are equipped with pressure transducer to check whether the flow rates are identical.

High-speed direct shadowgraph system is used to visualize the aircore inside the pressure swirl atomizer and the resulting hollow cone spray. Two high-speed cameras are used in sync mode for the visualization. One camera (Camera2) equipped with a 60 mm 1:2.8 D macro lens records the flow inside the pressure swirl atomizer and the other one (Camera1) equipped with a 24-85 mm 1:2.8-4d lens records the resulting hollow cone spray. The backlight illumination of the atomizer is achieved by using a light emitting diode (LED) whose light intensity can be adjusted. A set of collimating optics (a condenser lens and a Fresnel lens) delivered the green light from LED to the atomizer. The backlight illumination of the spray is obtained with a halogen lamb and a diffuser screen. Light sources and the cameras are aligned at the opposite sides as shown in Figure 2a. The effective image areas for Camera1 and Camera2 are 576x464 pixels (115x92mm) and 768x368 pixels (28x13 mm), respectively. The frame rate for both cameras is 20 kHz. The images taken are processed with an image processing tool developed in-house.

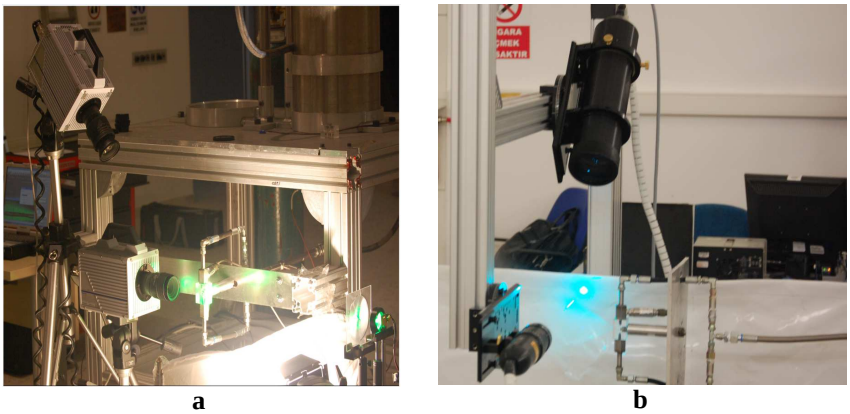

a b

Figure 2 a. High speed shadowgraphy setup on the atomizer test facility **b.** Phase Doppler Particle Analyzer.

The radial variation in Sauter mean diameter (SMD) is measured at one axial location with a commercial Phase Doppler Particle Analyzer (PDPA). The PDPA system is composed of an Ar-Ion laser, a multicolor beam separator, a transmitter, a receiver and a signal processor. The receiver and transmitter are positioned on a 3-axis traverse in a 43^{o} forward scatter configuration.

Numerical Method

Two-phase flow fields within the pressure swirl atomizer are computed using commercially available ANSYS-FLUENT software. Three dimensional (3D) and two-dimensional axis-symmetric swirl (2D-AXS) flow simulations are performed. In 2D-AXS flow simulations, all three velocity components are considered in the solution of conservation of momentum equations in axial, radial and tangential directions with the assumption of zero velocity gradients in tangential direction. The computational grid used in 2D-AXS simulations is shown in Figure 3a. In 2D-AXS flow solutions the 3D inlet boundary conditions are implemented by setting the radial velocity component such that the mass flow rate is satisfied. The tangential velocity component is set to the mean velocity in the tangential inlet port to ensure that same angular momentum enters the swirl chamber [14]. No-slip boundary conditions are applied at the wall boundaries and the pressure outlet boundary condition is applied at the outer boundaries. The computational grid used in 3D flow simulations are given in Figure 3b. Using the advantage of periodicity of the flow, only the upper half of the atomizer is modeled and the periodic boundary condition is applied to the boundary shown in dark blue in Figure 3b. The mass flow inlet boundary condition is applied at the tangential inlet. Pressure outlet boundary conditions are applied at the outer boundaries. The computational grid is hybrid; it contains tetrahedral elements at the tangential passage and at a small volume on swirl chamber adjacent to the tangential passage. In the remaining parts the grid contains hexahedral elements.

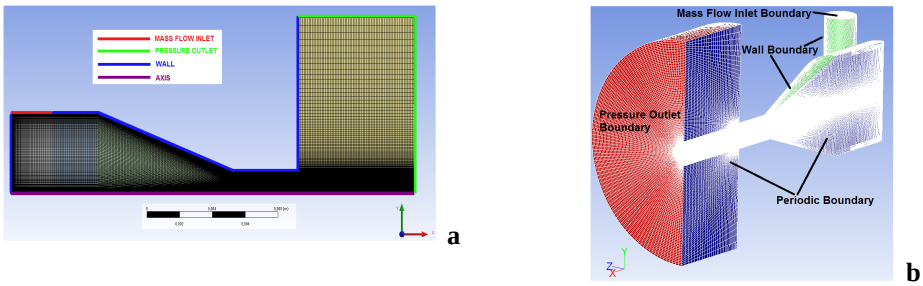

a b

Figure 3 Computational grids for **a.** 2D-AXS simulations **b.**3D flow simulations.

Results and Discussion

Experimental Results

Measurement of aircore diameter

The flow rate of water through the atomizer is adjusted by using the needle valve. The pressure drop across the atomizer is measured as 6.87 bars at water flow rate of 3.18x10^{-3} m^{3}/min. The aircore formed inside

the atomizer is visualized as shown in Figure 5. The aircore inside the pressure swirl atomizer resembles a drilling bit. Surface waves as well as vorticity waves on the aircore surface can be discerned (Figure 4). The aircore diameter is minimum at the base of the swirl chamber and it is almost constant along the swirl chamber up to the nozzle inlet where it starts growing in size. The aircore diameter is also not constant along nozzle. It first shows a gradual increase up to the mid nozzle location and then relatively sharp increase after mid nozzle. It attains its maximum value at the nozzle exit.

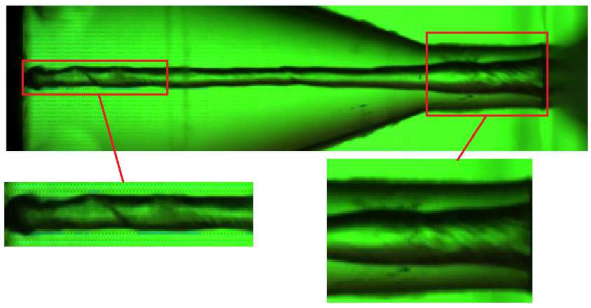

Figure 4 Snapshot of aircore.

Before each test, a fine needle of known diameter is inserted into the atomizer and a calibration image is captured. Conversion factor for the conversion from image (pixel) to physical (mm) coordinates is determined with the diameter of the fine needle. The quantitative values of the aircore diameter are obtained using the developed image processing tool. The image processing consists of converting the movie file to image files (Figure5a), converting the RGB image to grayscale image (Figure5b), subtracting the background image and increasing the intensity, if necessary, and finding the edges using the Sobel filter (Figure5c).

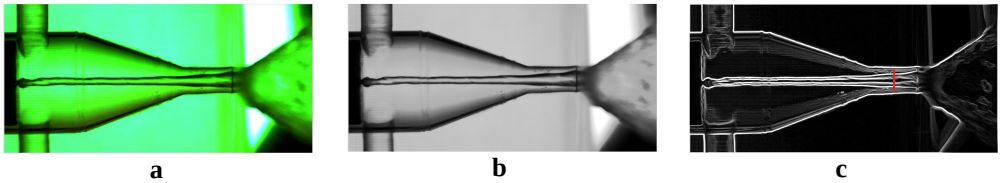

a **b** **c**

Figure 5 Image processing.

The intensity peaks are identified along the line drawn at the measurement location (red line in Figure5c) for each image and the aircore diameter is then found by calculating the distance between the intensity peaks which occurs at water-air interface. The time history of the measured aircore diameter at mid-nozzle is given in Figure 6a. The mean air core diameter at the measurement location is evaluated as 1.08 mm which is 0.07 mm smaller than the measurement of Dash et.al.[14].

The mean aircore diameter at the exit of the atomizer is evaluated as 1.24 mm. The aircore diameter at the exit of the atomizer can also be estimated based on the geometrical and physical parameters as follows [8],

$$d_{ac} = d_o - 2t$$

$$t = 3.66 \left[\frac{\mu_L d_o \dot{m}}{\rho_L \Delta P}\right]^{0.25} \quad (1)$$

where d_{ac} is the aircore diameter, d_o is the nozzle exit diameter, t is the liquid film thickness at the nozzle exit, ρ_L is the density of the liquid, μ_L is the dynamic viscosity of the liquid, ΔP_L is the pressure drop across the atomizer, $\dot{m}$ is the mass flow rate across the atomizer. The calculation of the aircore diameter at the nozzle exit using Equation 1 with the measured parameters gives 1.18 mm which is 0.06 mm lower than the measured aircore diameter at the exit of the atomizer. The spectral analysis of the aircore diameter data reveals a dominant frequency at 273Hz (Figure 6b).

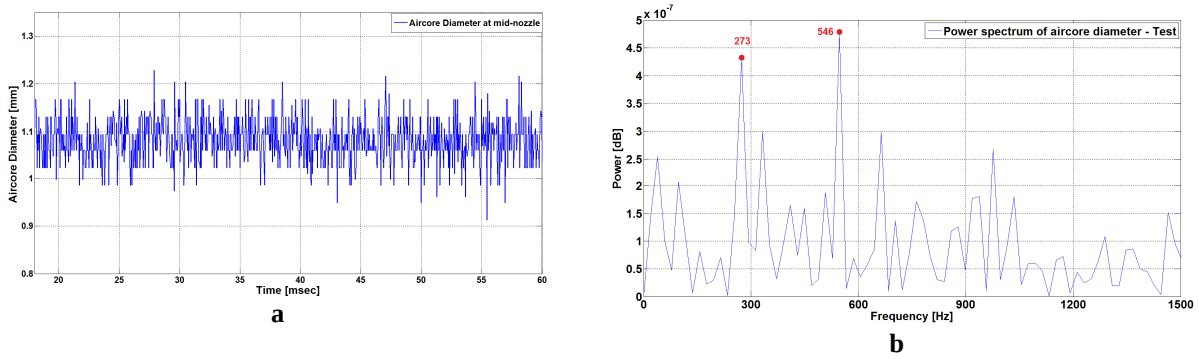

Figure 6 a. Time history of the aircore diameter at mid-nozzle, **b.** Power spectrum of aircore diameter.

Measurement of spray cone angle

Spray cone angle is measured using the images taken by Camera1 (Figure 7a). A calibration image is taken before each test. The quantitative values for the spray cone angle are obtained with the developed image processing tool. The similar image processing steps taken in the aircore diameter measurement are followed in order to find the edges of the spray cone.

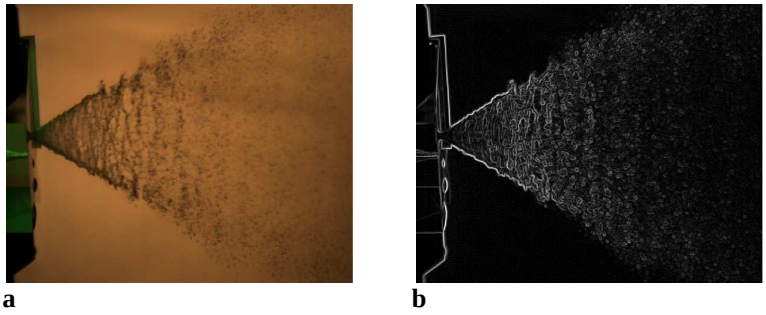

Figure 7 Measurement of spray cone angle **a.** RGB image **b.** Image with edges.

The two intensity peaks which occur at the spray boundary are identified and the radial distance between the two intensity peaks is calculated for each image at 13 mm away from the atomizer exit. The spray half cone angle is then calculated using the calculated radial distance and the known axial position of the measurement location. The mean half spray cone angle, which is calculated by averaging instantaneous spray cone angle measurements for 1333 images, is found to be 33^o. The measured mean half spray cone angle is 4^o larger than the measurement done by Dash et.al. [14].

Measurement of Sauter mean diameter

The Sauter mean diameter (SMD) of the resulting spray can be estimated using the empirical equation of Wang and Lefebvre [9]

$$SMD = 4.52\left(\frac{\theta\mu_L^2}{\rho_A\Delta P_L^2}\right)^{0.25}(tcos\theta)^{0.25} + 0.39\left(\frac{\rho_L}{\rho_A\Delta P_L}\right)^{0.25}(tcos\theta)^{0.75} \quad (2)$$

where θ is the spray cone angle, ρ_A is the density of the ambient medium, ρ_L is the density of the liquid, μ_L is the dynamic viscosity of the liquid, ΔP_L is the pressure drop across the atomizer and t is the film thickness at the nozzle exit. The calculation of the SMD using Equation (2) with the measured parameters provides an SMD value of 225 micrometers (μm).

The variation in SMD along the radial location at 112 mm downstream of the atomizer is given Figure 8. The radial distribution of the SMD reveals that the small droplets present near the atomizer axis and as one move away from the atomizer axis the SMD increases and reaches to maximum value of 213 μm. at r=70 mm.

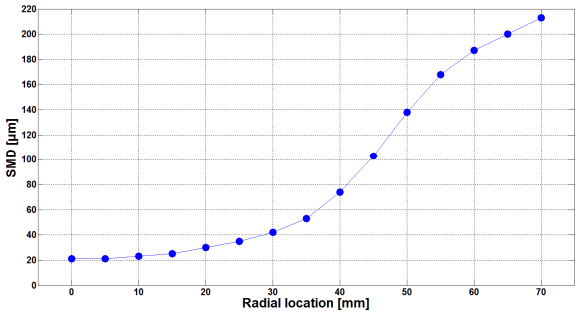

Figure 8. Variation in SMD along radial location.

Numerical Results

3D and 2D-AXS unsteady flow simulations are performed with ANSYS-FLUENT CFD software. Unsteady laminar Navier-Stokes equations are solved for incompressible phases using the pressure based coupled algorithm, which solves a coupled system of momentum and pressure based continuity equations. Second order upwind scheme is selected for the solution of momentum equations. Pressure Straggered Option (PRESTO) scheme is employed for the computation of face pressures. Volume of fluid method with High Resolution Interface Capturing scheme (HRIC) scheme is used for the treatment of two phase flow, which solves the volume fraction of each phase in the computational cells. In order to take into account the surface tension along each phase, continuum surface force (CSF) model is used. The unsteady simulations are first order accurate in time with a fixed time step of 0.5 microseconds (µsec) for 2D-AXS and 10 µsec. for 3D numerical simulations.

For 2D-AXS flow simulations the mass flow inlet boundary condition is applied to a line which extends 2.49 mm from the base of the swirl chamber. Mass flow rate of 0.053 kg/s is defined at the inlet boundary along a direction vector of -0.1572j+0.9866k, where j and k are the unit vectors along radial and tangential directions respectively. The solution domain is extended up to 7 mm downstream and 8 mm in radial direction. The two dimensional computational grid contains 31900 quadrilateral elements (Figure3). The major characteristics of the 2D-AXS solution domain and the grid density are extended to third dimension in 3D numerical simulations. The computational domain is extended 7 mm downstream and 8 mm in y and z directions and computational grid contains 1,800,000 mixed elements.

The mean pressure drop across the atomizer is predicted as 8.8 and 8.1 bars and the half spray cone angle is predicted as 28.5^{o} and 29^{o} for 2D-AXS and 3D numerical simulations respectively. Both 2D-AXS and 3D numerical simulations capture free surface deflections at the base of the swirl chamber. In 2D-AXS numerical simulations, abrupt free surface deflections are predicted at the base of the swirl chamber, which causes fluctuations (surface waves) on the aircore (Figure9a). In 3D simulations vorticity waves are identified at the air-water interface in addition to surface waves.

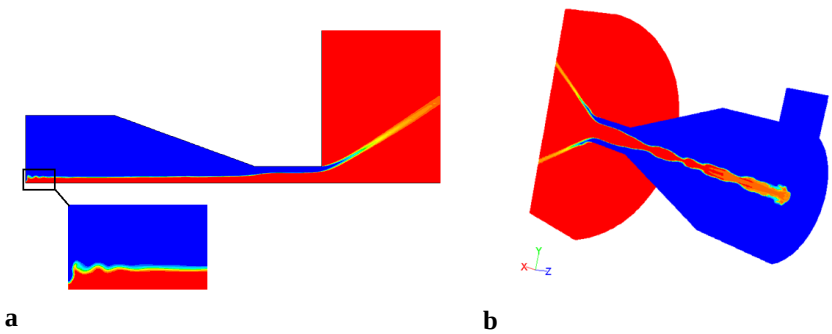

Figure 9a. Contours of air volume fraction (2D-AXS), **b.** Contours of air volume fraction (3D)

Aircore fluctuations at mid nozzle are evaluated by using the predicted volume fraction of air for both 2D-AXS and 3D numerical simulations. The radial variation of air volume fractions are evaluated at mid-nozzle for 2D-AXS numerical simulations. On the other hand, the radial variations of air volume fractions are evaluated at mid-nozzle in a plane perpendicular to periodic boundaries for 3D numerical simulations. The radial profile of air volume fraction at mid nozzle at a single time instant is given in Figure10. The aircore diameter values at mid nozzle are calculated by using the predicted volume fraction values.

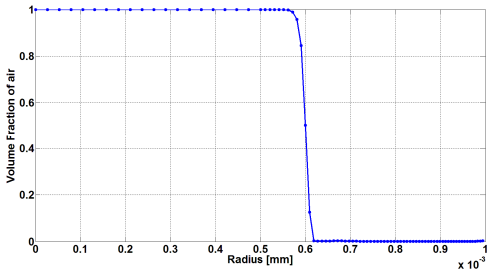

Figure 10. Radial profile of air volume fraction at mid nozzle.

The unsteady aircore diameter, predicted by 2D-AXS and 3D numerical simulations, are given in Figure11a and Figure11b, respectively. The unsteady aircore diameter contains 1024 data points sampled at 20 kHz. The mean aircore diameter at mid nozzle is predicted as 1.128 mm and 1.19 mm for 3D and 2D-AXS numerical simulations respectively. The results of the spectral analysis of the predicted aircore data is shown in Figure 11c and Figure11d, which gives dominant frequency at 214 Hz.

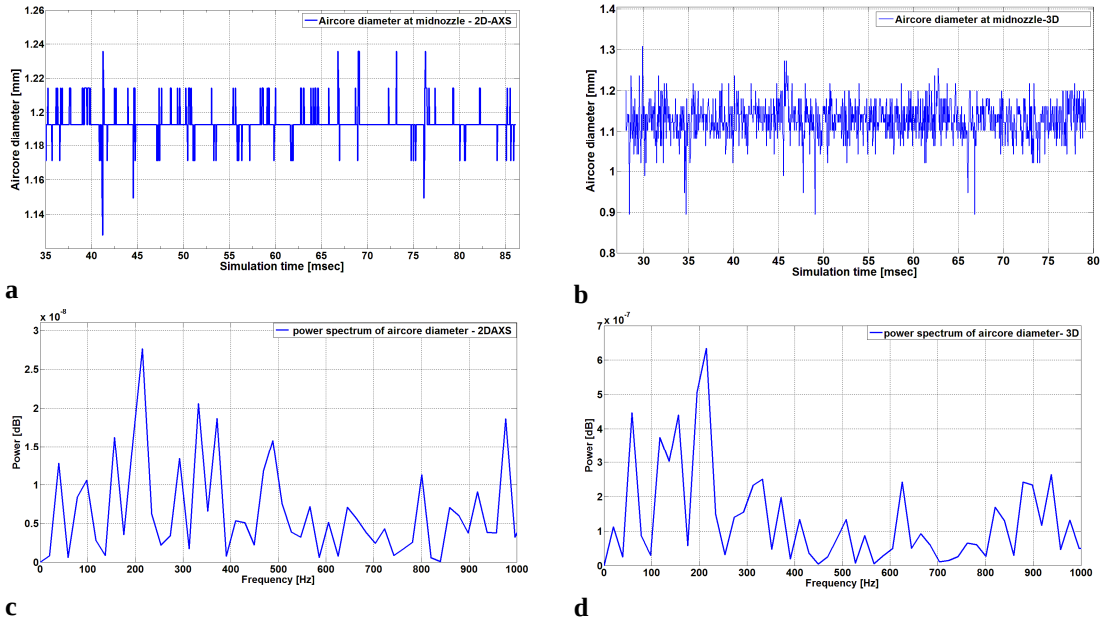

Figure11 a. Aircore diameter (2D-AXS simulations) **b**. aircore diamater (3D simulations) **c**. power spectrum of aircore diameter (2D-AXS simulations) **d**. power spectrum of aircore diameter (3D simulations).

Both 3D and 2D-AXS numerical simulations shows fairly good agreement with test results in terms of aircore diameter and spray cone angle. However the predicted pressure drop values are higher for both simulations when compared to the experiment. The 3D and 2D-AXS numerical simulations give detailed information about the flow field inside the atomizer as well as the resulting spray cone angle. The CFD simulations shows two vortices at the base of the swirl chamber near the aircore interface which may explain the presence of the surface waves created along the aircore interface.

Summary and Conclusions

In this study the unsteady flow fields in a pressure swirl atomizer is studied experimentally and numerically. The critical flow parameters such as the aircore diameter, the spray cone angle and the pressure drop across the atomizer are evaluated for a constant mass flow rate. The unsteady fluctuations on the aircore diameter are assessed in both experimental and numerical studies. The obtained mean values of these parameters agree well with the findings of other researchers [8, 9, and 14]. The fluctuation frequencies of the aircore diameter are also obtained by spectral analysis of the time resolved data. The results obtained indicate that the high speed shadowgraphy method can be used to measure the dynamic characteristics of the aircore inside a real scale atomizer. The numerical simulations show that the flow inside the pressure swirl atomizer can be assessed by using

CFD techniques. Such techniques can be used during the preliminary design stage of pressure swirl atomizers in determining the main geometrical parameters and exploring the unsteady flow fields.

Acknowledgements

This study has been supported by TÜBİTAK-SAGE under Project IBTA founded by State Planning Organization of Turkey.

References

[1] Lefebvre A.H., *Atomization and Sprays*, CRC Press, Florida, 1989, ISBN 0-891116-603-3, pp 1.
[2] Bavyel L., Orzechowsk Z., *Liquid Atomization*, Taylor & Francis, Washington, DC, 1993, ISBN 0-89116-959-8.
[3] Bazarov V., Yang V., Puri P., *Design and Dynamics of Jet and Swirl Injectors*, Book Chapter in Liquid Rocket Thrust Chambers: Aspects of Modeling, Analysis and Design, AIAA, Volume 200, Progress in Astronautics and Aeronautics, 2004, ISBN 1-56347-223-6.
[4] Abramovich G.N., *The Theory of Swirl Atomizer*, Industrial Aerodynamics, BNT ZAGI, Moscow, pp. 114-121, 1944.
[5] Taylor G.I., *The Mechanics of Swirl Atomizers*, vol.2 pt. 1, International Congress of Applied Mechanics, London. 1948.
[6] Giffen E., Muraszew A., *Atomization of Liquid Fuels*, Chapman and Hall, London, 1953.
[7] Som S.K., Mukherjee S.G., *Theoretical and Experimental Investigations on the Formation of Air Core in a Spray Atomizing Nozzle*, Applied Scientific Research, 36,pp. 173-196,1980.
[8] Suyari M., Lefebvre A.H., *Film Thickness Measurement s in a Simplex Swirl Atomizer*, AIAA Journal of Propulsion, Vol. 2, No. 6, Nov.-Dec. 1986.
[9] Wang X.F., Lefebvre A.H., *Mean Drop Sizes from Pressure-Swirl Nozzles*, AIAA Journal of Propulsion, Vol. 3, No. 1, Jan.-Feb. 1987.
[10] Ballester J., Dopazo C., *Discharge Coefficient and Spray Angle Measurements for Small Pressure Swirl Nozzles*, Atomization and Sprays, vol.4, pp. 351-367, 1994.
[11] Chinn J.J., Yule A.J., De Keukelaere H.J.K., *Swirl Atomizer Internal Flow: A Computational and Experimental Study*, 12th Annual Conference of ILASS-Europe, Lunf, Sweden, June, 1996.
[12] Datta A., Som S.K., *Numerical Prediction of Air Core Diameter, Coefficient of Discharge and Spray Cone Angle of a Swirl Spray Nozzle*, International Journal of Heat and Fluid Flow. Vol. 21 , pp. 412-419, 2000
[13] Sakman A.T., Jog M.A., Jeng S.M., Benjamin M.A., *Parametric Study of Simplex Fuel Nozzle Internal Flow and Performance*, AIAA Journal, Vol. 38, No.7, 2000.
[14] Dash S.K., Halder M.R., Peric M., Som S.K., *Formation of Air Core in Nozzles with Tangential Entry*, ASME Journal of Fluids Engineering, Vol. 123, pp. 829-835, 2001.
[15] Cooper D., Yuke A.J., *Waves on the Air Core/liquid Interface of a Pressure Swirl Atomizer*, ILASS-Europe, Zurich, September 2001.
[16] Von Lavante E., Maatje U., Albina F.O., *Investigation of Unsteady Effects in Pressure Swirl Atomizers*, ILASS-Europe, Zaragosa, September 2002.
[17] Donjat D., Estivalezes J-L., Michau M., Lavergne G., *Phenomenological Study of the Pressure Swirl Atomizer Internal Flow*, 9th International Conference on Liquid Atomization and Spray Systems, July 13-17,2003, Sorrento, Italy.
[18] Chinn J.J., Cooper D., Yule A.J., *A Comparison of Analytically and Experimentally Determined Wave Parameters on the Liquid Interface of the Aircore of a Swirl Atomizer*, 19th Annual Meeting of ILASS (Europe) ,6-8 September 2004, Nottingham, United Kingdom.
[19] Halder M.R , Som S.K., *Numerical and Experimental Study on Cylindrical Swirl Atomizers*, Atomization and Sprays, Vol.16, pp. 223-236, 2006.
[20] Marchione T, Allouis C., Amoresane A., Berreta F., *Experimental Investigation of a Pressure Swirl Atomizer Spray* ,Journal of Propulsion and Power, Vol.23, No. 5, pp.1096-1101, 2007.
[21] Hinekel J.N., Villa Nova H.F., Bazarov V.G., *CFD Analysis of Swirl Atomizers*, 44th AIAA/ASME/SAE/ASEE Joint Propulsion Conference and Exhibit, Hartford, CT, 21-23 July 2008.
[22] Kim S., Khil T., Kim D., Yoon Y., *Effect of Geometry on the Liquid Film Thickness and Formation of Air Core in a Swirl Injector*, Measurement Science and Technology, Vol. 29 , pp. 1-11,2009.
[23] Lee E.J., Oh S.Y., Kim H.Y., James S.C., Yoon S.S., *Measuring Aircore Characteristics of a Pressure-Swirl Atomizer via a Transparent Acrylic Nozzle at Various Reynolds Numbers*, Experimental Thermal and Fluid Science,34, 2010,1475-1483.
[24] Fu Q.,Yang l., Qu Y., *Measurement of Annular Liquid Film Thickness in an Open-End Swirl Injector*, Aerospace Science and Technology, 15, 2011, 117-124.